Anisotropic magnetoresistance and anomalous Hall effect in manganite thin films

2005 J. Phys.: Condens. Matter 17 2733

(http://iopscience.iop.org/0953-8984/17/17/022)

INSTITUTE OF PHYSICS PUBLISHING JOURNAL OF PHYSICS: CONDENSED MATTER

J. Phys.: Condens. Matter **17** (2005) 2733–2740 doi:10.1088/0953-8984/17/17/022

Anisotropic magnetoresistance and anomalous Hall effect in manganite thin films

M Bibes[1,2], V Laukhin[1,3], S Valencia[1], B Martínez[1], J Fontcuberta[1], O Yu Gorbenko[4], A R Kaul[4] and J L Martínez[5]

[1] Institut de Ciència de Materials de Barcelona, CSIC, Campus de la UAB, 08193 Bellaterra, Spain
[2] Institut d'Electronique Fondamentale, Université Paris-Sud, 91405 Orsay, France
[3] Institució Catalana de Recerca i Estudis Avançats, Passeig Lluís Companys 23, 08010 Barcelona, Spain
[4] Department of Chemistry, Moscow State University, 119899 Moscow, Russia
[5] Instituto de Ciencia de Materiales de Madrid, CSIC, Cantoblanco, 28049 Madrid, Spain

Received 27 September 2004, in final form 21 February 2005
Published 15 April 2005
Online at stacks.iop.org/JPhysCM/17/2733

Abstract

We report on anisotropic magnetoresistance (AMR) and Hall effect measurements along the $[1\bar{1}0]$ and [001] directions in a (110)-oriented $La_{2/3}Ca_{1/3}MnO_3$ thin film. While the electrical resistivity and the ordinary Hall coefficient are smaller for I along [001], evidencing some anisotropy of the Fermi surface, both the AMR and the anomalous Hall coefficient are larger when the current is applied along $[1\bar{1}0]$. Since these two phenomena originate from spin–orbit coupling effects, we state that our results support an anisotropy of the spin–orbit interaction in manganites. The possible origin of this anisotropy is discussed.

1. Introduction

Among magnetic oxides, mixed-valence manganites show a number of very interesting features, like colossal magnetoresistance or charge and orbital ordering [1]. In intermediate bandwidth compounds such as $La_{2/3}Ca_{1/3}MnO_3$, the electronic state shows a crossover between metallic behaviour at low temperature and polaronic state at temperatures above T_C, with the coexistence of both phases in a rather wide range of temperatures around T_C. In this regime, the application of a magnetic field favours the metallic phase with respect to the localized one, thus inducing a decrease of the resistivity: the so-called colossal magnetoresistance.

Anisotropic magnetoresistance AMR (the difference observed in magnetoresistance when the electric current I is applied parallel or perpendicular to the magnetization) is a feature of all metallic ferromagnets [3, 2] and is usually related to spin–orbit coupling accompanying a mixing of minority and majority spin states [4] or to quadrupole scattering [5]. In general, as

for the temperature dependence, the AMR behaves like the square of the magnetization [6]. In manganites, AMR has been studied by a few groups [7–9, 11, 10] and one puzzling feature is that the temperature dependence of the AMR shows a peak close to T_C [9, 11, 10]. Moreover, the shape of the AMR amplitude versus temperature curves appears to be affected by the crystalline quality of the samples and can be qualitatively interpreted by the sum of two contributions, one following the magnetization and one showing a peak close to the Curie temperature [11, 12]. This intrinsic behaviour has been related to the spin–orbit interaction but a quantitative understanding is still lacking [13].

Another interesting magnetotransport phenomenon is the anomalous Hall effect (AHE) which appears in addition to the ordinary Hall effect (OHE) in ferromagnets. The total Hall resistivity can then be written:

$$\rho_H = \rho_{OHE} + \rho_{AHE} = R_{OHE} B + \mu_0 R_{AHE} M \tag{1}$$

where ρ_{OHE} and ρ_{AHE} are the ordinary and anomalous contributions to the Hall resistivity, with R_{OHE} and R_{AHE} the ordinary and anomalous Hall coefficients, respectively, B is the magnetic induction and μ_0 is the vacuum permeability.

In standard magnetic metals, the AHE arises from an asymmetry in the right–left scattering of the conduction electrons induced by skew-scattering or side-jump processes that depend on the spin–orbit interaction [14]. In manganites, the sign and magnitude of R_{AHE} stand in contradiction to these conventional theories. Its temperature dependence was found to peak close to T_C by several groups [15–17]. Recently two new models have appeared proposing an explanation for the AHE in manganites [18, 19]. Both suggest that its origin resides in spin–orbit assisted quantal phase effects. The main difference in these two models is that Lyanda-Geller *et al* [18] consider conduction between localized states in the polaronic regime whereas Calderón and Brey [19] use a double-exchange Hamiltonian that does not provide localization at high temperatures. In both models, the AHE is found to depend linearly upon the spin–orbit interaction constant λ_{so}.

2. Experimental details

We have performed AMR and Hall effect measurements on a 300 nm thick (110)-oriented $La_{2/3}Ca_{1/3}MnO_3$ epitaxial thin film grown by metal-organic chemical vapour deposition (MOCVD) on $SrTiO_3$(110) (all crystallographic directions are indexed in the pseudo-cubic unit-cell). The crystalline quality of the sample was checked by x-ray diffraction and the film was found to be fully (110)-oriented with a cube-on-cube epitaxy. The x-ray study confirmed that the [001] and [$1\bar{1}0$] directions are contained in the plane of the film and parallel to its edges. The out-of-plane parameter c was 3.857 ± 0.002 Å and the in-plane parameter (as determined from a set of symmetrical and asymmetrical reflections in the $2\theta = 20°$–$120°$ range) $a = 3.868 \pm 0.003$ Å. Although the difference between a and c is somewhat slightly larger than the splitting of the cell parameters in the orthorhombic $Pnma$ structure ($c = 3.863$ Å and $a = 3.869$ Å), the film can be considered as virtually relaxed.

The sample was patterned by optical lithography and chemical etching into two six-contact 150 μm wide tracks, one being parallel to the [001] direction and the other one parallel to the [$1\bar{1}0$] direction.

The AMR measurements were performed in a Quantum Design PPMS equipped with a sample rotator that enabled varying the angle θ between the magnetic field and the current in the film plane; $\theta = 0$ corresponds to the field applied perpendicular to the current. The Hall voltage was measured in a four-contact configuration [20] in the PPMS using a lock-in voltmeter. To cancel the effect of the field on the longitudinal component of the resistivity

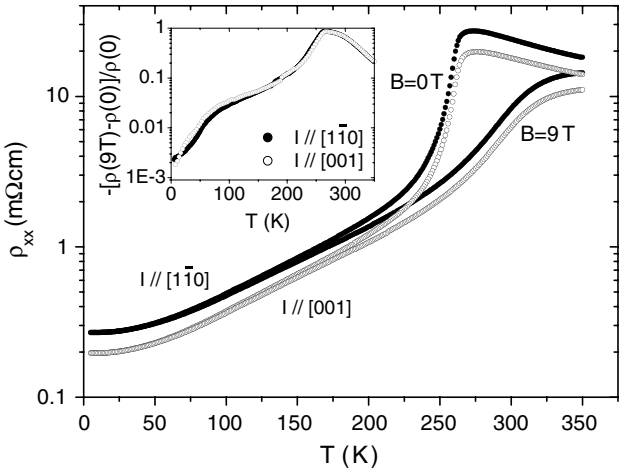

Figure 1. Temperature dependence of the resistivity of the film for I applied along either [1$\bar{1}$0] (solid symbols) or [001] (open symbols), at zero field and 9 T. Inset: temperature variation of the normalized difference between the resistivity with and without field, for the two current directions.

contributing to the measured voltage, we swept the field to positive values and then to negative values and defined the Hall signal as half the difference between the signals measured at positive and negative fields.

3. Results and discussion

In figure 1 we show the temperature dependence of the longitudinal resistivity (ρ_{xx}) at zero field and 9 T, for I applied along [1$\bar{1}$0] and [001]. In all the temperature range, the resistivity is larger by about a factor 1.4 when I is applied along [1$\bar{1}$0] than for I along [001]. However, the metal-to-insulator transition (T_P) temperature ($T_P = 270$ K) and the magnetoresistance (see inset of figure 1) show little influence of the current direction. T_P is very close to the Curie temperature $T_C = 275$ K for this sample. These results are in good agreement with those of Amaral *et al* [10] who also explored transport properties along different directions in a (110)-oriented LCMO film and found $\rho_{[1\bar{1}0]}/\rho_{[001]} \simeq 1.2$.

The AMR was measured for fields up to 9 T and in the 10–310 K temperature range. Low-field measurements did not show any four-fold contribution which confirmed the uniaxial symmetry of the film. The angular dependence of the magnetoresistance defined at 5 T as:

$$\Gamma = [R(5\ \mathrm{T}, \theta) - R(5\ \mathrm{T}, \theta = 0)]/R(5\ \mathrm{T}, \theta = 0) \tag{2}$$

could be fitted by:

$$\Gamma = A_1 \cos(2\theta + A_2) + A_0 \tag{3}$$

where A_1 corresponds to half the amplitude of the angular dependence of the magnetoresistance, A_2 is a phase parameter (close to 0 and accounting for sample misalignment) and A_0 an offset. All these parameters are in general temperature and field dependent. However, the resistance was found to be always larger when the field was applied perpendicular to the current ($\theta = 0$) in agreement with other studies [9, 11].

Some examples of the angular dependence of the magnetoresistance measured at high field (5 T) are presented in figure 2. Clear oscillations of period 180° are detected, as expected

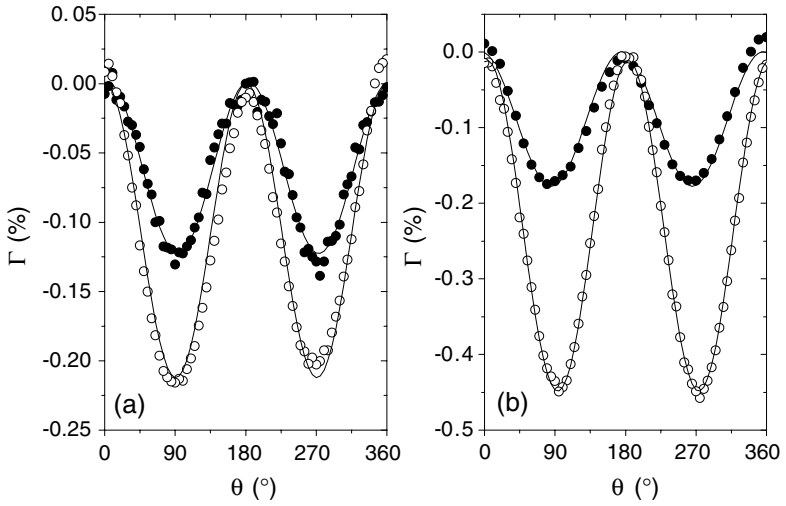

Figure 2. Angular variation of the magnetoresistance at 5 T for measurements with I parallel to [001] at 10 K (solid symbols) and 250 K (open symbols) (a) and I parallel to $[1\bar{1}0]$ (b) at 10 K (solid symbols) and 290 K (open symbols).

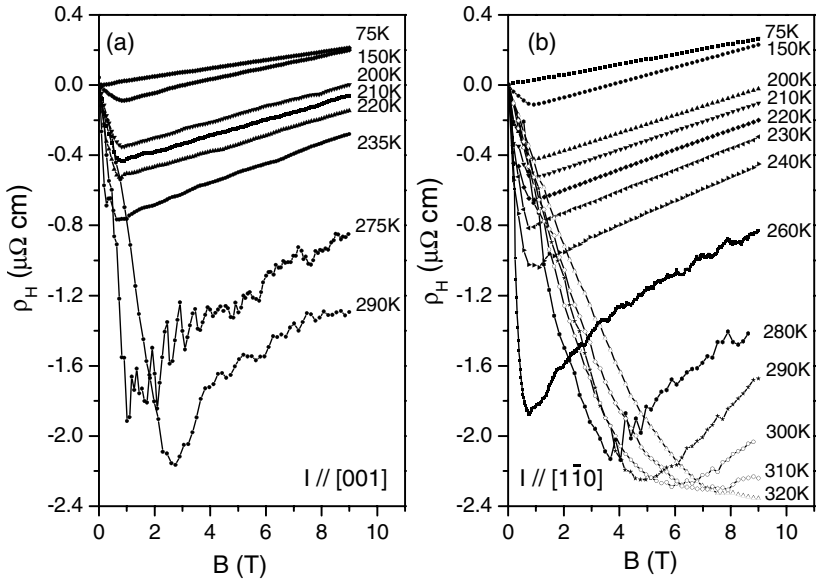

Figure 3. Hall resistivity with I applied along [001] (a) and $[1\bar{1}0]$ (b).

for a measurement under a saturating magnetic field, its amplitude being dependent on the temperature and on the direction of the electric current. This will be discussed later on.

The field and temperature dependence of the Hall resistivity ρ_H is shown in figure 3. At low temperature ($T < 100$ K), for both current directions a linear behaviour is obtained which has to be ascribed to the OHE only since no magnetization-like low-field variation is observed. The sign of R_{OHE} indicates that the charge carriers are holes in agreement with the doping value and results of the literature.

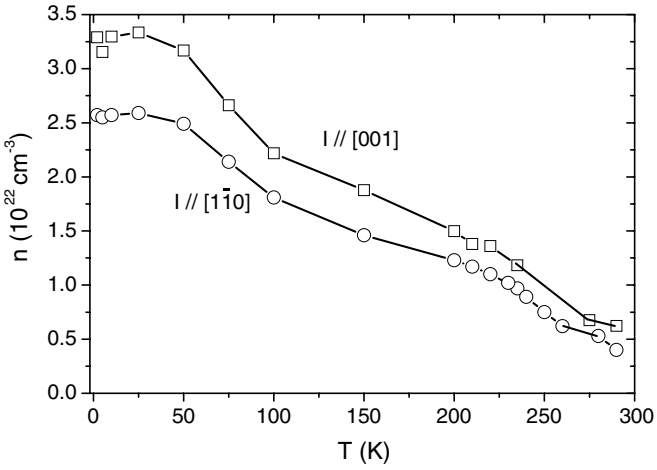

Figure 4. Number of carriers as deduced from R_{OHE} in the free electron model.

At higher temperatures ($T > 100$ K), a low-field decrease of ρ_{H} is detected signalling the rising contribution of the AHE. The OHE and AHE coefficients have opposite sign, as previously reported [15, 16]. However, the accurate separation of both components is not an easy task as suggested in [18]. This is particularly difficult at temperatures close to the Curie temperature where the low-field transverse Hall voltage can be masked by non-intrinsic effects [21, 22]. However, we can tentatively distinguish two methods to extract the AHE at temperatures lower than T_{C}: one consists in dividing the low-field slope of the Hall resistivity by the low-field slope of the magnetization M (measured with the field applied perpendicular to the film plane), that is:

$$R_{\mathrm{AHE}} = \frac{\partial \rho_{\mathrm{AHE}}/\partial H}{\partial M/\partial H} \simeq \frac{\partial \rho_H/\partial H}{\partial M/\partial H} \tag{4}$$

and the other one in extrapolating the high-field slope of $\rho_{\mathrm{H}}(H)$ to zero and dividing by the saturation magnetization. We have used both techniques to determine the AHE coefficient R_{AHE} and observed that its temperature dependence is roughly the same in both cases.

The OHE coefficient R_{OHE} is calculated from the slope of the high-field Hall resistivity (like Jakob *et al* [16] we make the assumption that the magnetization is almost independent of field in this regime as suggested by the linearity of the high-field Hall resistivity even close to T_{C}). From this OHE coefficient we can calculate the effective charge carrier concentration in the free-electron model ($n = (e R_{\mathrm{OHE}})^{-1}$, e being the charge of the electron). We plot the carrier density (note that $R_{\mathrm{OHE}} > 0$ and thus the transport is hole-dominated) versus temperature for both current directions in figure 4. The density of carriers decreases with temperature but does not vanish at T_{C}. Rather, if the data are extrapolated to higher temperatures, it appears that n would become zero around 330 K. This may be related to the percolative nature of the metal-to-insulator transition in LCMO. At 10 K, the values we obtain correspond to 1.9 carriers per Mn ion for I along [001] and 1.5 carriers per Mn ion for I along [1$\bar{1}$0]. These values are much larger than the expected value ($n \simeq x \simeq 0.33$), which is a frequent trend in the literature. The difference observed between the [001] and [1$\bar{1}$0] directions indicates some anisotropy of the Fermi surface of LCMO.

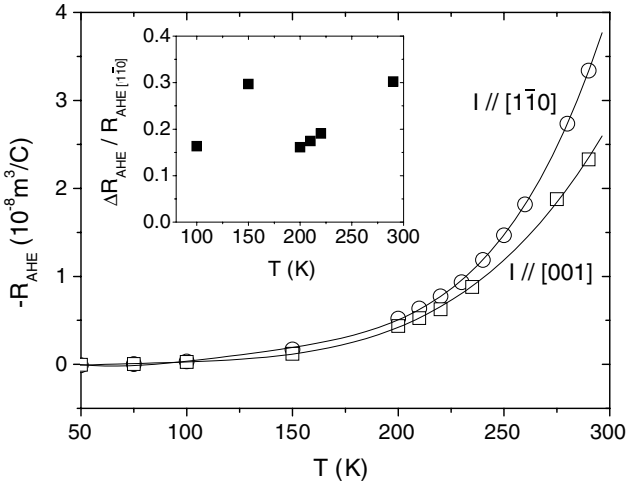

Figure 5. Temperature dependence of the AHE coefficient for both current orientations. Inset: temperature dependence of the difference ΔR_{AHE} between the AHE coefficient for I along $[1\bar{1}0]$ and I along [001], normalized by $R_{\mathrm{AHE}[1\bar{1}0]}$.

Alternatively, if the two-band model is used, the OHE coefficient is related to the densities n and mobilities μ of holes (h) and electrons (e):

$$R_{\mathrm{OHE}} = \frac{n_{\mathrm{h}}\mu_{\mathrm{h}}^2 - n_{\mathrm{e}}\mu_{\mathrm{e}}^2}{e(n_{\mathrm{h}}\mu_{\mathrm{h}} + n_{\mathrm{e}}\mu_{\mathrm{e}})^2}. \tag{5}$$

Following Jakob *et al* [16] and using the Fermi surface calculation of Pickett and Singh [23] (a Γ-centred electron pocket with 0.05 electron per unit cell and R-centred hole pocket with 0.55 hole per unit cell), we can deduce the mobility ratios $\mu^\star = \mu_{\mathrm{e}}/\mu_{\mathrm{h}}$ for the current applied in both directions: $\mu^\star_{[1\bar{1}0]} = 2.26$ and $\mu^\star_{[001]} = 2.48$. These values are in good agreement with those previously reported [16]. Again, these data suggest that the electron and/or hole Fermi surface present some anisotropy, which has not yet been reported for LCMO.

The AHE coefficient R_{AHE}, extracted by extrapolating the high-field slope of $\rho_{\mathrm{H}}(H)$ to zero and dividing by the saturation magnetization, is plotted in figure 5. For both current directions, R_{AHE} increases with temperatures up to $T = 290$ K, the maximum temperature at which the AHE contribution could be safely extracted, so that we cannot make any conclusions concerning the possible presence of a maximum in its variation with temperature, as claimed by Yang *et al* [24] and Matl *et al* [15]. However, we must mention that the extraction of the AHE coefficient at higher temperatures is problematic due to the large magnetic susceptibility of the film, and to the resulting difficulty in estimating the OHE coefficient unless extremely high fields were used. In any event, the behaviour we find, i.e. an increase of R_{AHE} with temperature up to T_{C} is indeed in agreement with previous reports [25, 26]. In the temperature range where R_{AHE} can be extracted, we observe that it is larger for I parallel to $[1\bar{1}0]$ than for I parallel to [001], in the whole temperature range, by about 23% (see inset of figure 5). This difference can arise from various contributions. In the model of Lyanda-Geller *et al* [18], the anomalous Hall resistivity is written:

$$\rho_{\mathrm{AHE}} = -\frac{1}{ne}\left(\frac{\alpha\hbar\zeta}{ed^2\cos^4(\Theta/2)}\right) \tag{6}$$

where ζ is an asymmetry parameter involving the magnetization, the area defined by the position of the three sites between which the electron is hopping and the spin–orbit coupling

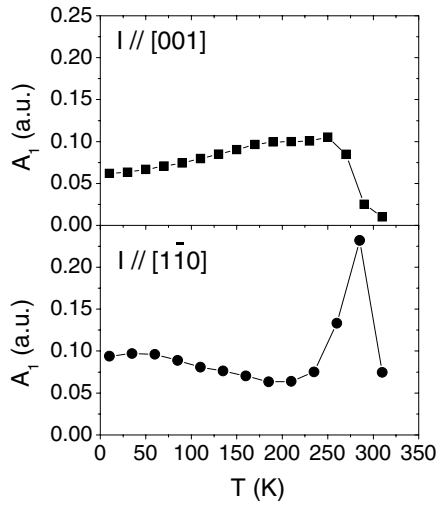

Figure 6. Temperature dependence of the A_1 coefficient for both current orientations.

constant, α is a numerical factor describing the multiplicity of the carrier-phonon interference processes and the difference between nearest neighbour and next-nearest neighbour hopping amplitude ($\alpha \simeq 2.5$) [18], d is the distance between Mn sites and Θ is the average misorientation angle between adjacent spins. We are applying this model rather than that of Calderón and Brey [19] because, as we have already mentioned, our $La_{2/3}Ca_{1/3}MnO_3$ film shows a high-temperature metal-to-insulator transition and so a polaronic treatment seems more appropriate. In this model, ζ depends linearly on λ_{so} and therefore so does ρ_{AHE}. Anisotropy parameters are thus λ_{so} and d, so that we can write:

$$\frac{\rho_{AHE[001]}}{\rho_{AHE[1\bar{1}0]}} = \frac{\lambda_{so[001]}}{\lambda_{so[1\bar{1}0]}} \frac{d^2_{[1\bar{1}0]}}{d^2_{[001]}}. \tag{7}$$

When I runs along $[1\bar{1}0]$, $d = a\sqrt{2}$ (a being the unit cell parameter) while when I is applied along [001], $d = a$. From equation (4) and assuming that R_{AHE} does not dependent on magnetic field, we have:

$$\frac{\rho_{AHE[001]}}{\rho_{AHE[1\bar{1}0]}} = \frac{R_{AHE[001]}}{R_{AHE[1\bar{1}0]}}. \tag{8}$$

As shown in the inset of figure 5, the difference ΔR_{AHE} between the AHE coefficient for I along $[1\bar{1}0]$ and I along [001], normalized by $R_{AHE[001]}$, takes values of 0.23 ± 0.07 between 100 and 300 K, that is $R_{AHE[001]}/R_{AHE[1\bar{1}0]} \simeq 0.7$–$0.8$. From equation (7) we thus find that the anisotropy in the spin–orbit interaction is $\lambda_{so[1\bar{1}0]} \simeq 2.8\lambda_{so[001]}$.

In figure 6 we plot the temperature dependence of the angular dependence of the AMR coefficient A_1 for I applied along [001] and along $[1\bar{1}0]$. We notice that, similar to what happens for R_{AHE}, A_1 for I parallel to $[1\bar{1}0]$ tends to be larger than its equivalent for I along [001]. The ratio between maximum values is about 2 and this maximum occurs at a temperature slightly lower when I is parallel to [001], close to the Curie temperature and the resistivity maximum.

As mentioned previously, the AMR originates in spin–orbit coupling effects and it is expected that a larger spin–orbit interaction may lead to a stronger AMR. In our case, in the transition regime, the AMR is stronger in the case of I along $[1\bar{1}0]$ in agreement with the value

on λ_{so} determined from AHE results. Therefore, these results point towards a same origin for the AMR and the AHE, in which the spin–orbit interaction is a key magnitude, and suggest that λ_{so} depends on the crystallographic direction.

This might be related to the increase of the Jahn–Teller distortion when the temperature approaches T_C. The anisotropic deformation of the MnO_6 octahedra may induce an anisotropy in the interaction of the spins with the e_g orbitals, since in this regime $d_{x^2-y^2}$ and d_{z^2} are no longer degenerate.

In summary, we have performed anisotropic magnetoresistance and Hall effect measurements with current along the [001] and [1$\bar{1}$0] directions of a (110)-oriented thin film of $La_{2/3}Ca_{1/3}MnO_3$. The amplitude of these two effects is larger when the current is applied along [1$\bar{1}$0], which is indicative of some anisotropy in the spin–orbit interaction, whose origin may reside in Jahn–Teller distortion effects, either of intrinsic nature or related to residual anisotropic strains. Systematic measurements on films with controlled strain levels are underway to better understand this point.

References

[1] Coey J M D, Viret M and von Molnàr S 1999 *Adv. Phys.* **48** 167
[2] Campbell I and Fert A 1982 Transport properties of ferromagnets *Ferromagnetic Materials* vol 3, ed E P Wohlfarth (Amsterdam: North-Holland)
[3] McGuire T and Potter R 1975 *IEEE Trans. Magn.* **11** 1018
[4] Malozemoff A P 1986 *Phys. Rev.* B **34** 1853
[5] Sablik M J, Pureur P, Creuzet G, Fert A and Levy P M 1983 *Phys. Rev.* B **28** 3890
[6] Stampe P A, Kunkel H P, Wang Z and Williams G 1995 *Phys. Rev.* B **52** 335
[7] Eckstein J N, Bozovic I, O'Donnell J, Onellion M and Rzchowski M S 1996 *Appl. Phys. Lett.* **69** 1312
[8] O'Donnell J, Onellion M, Rzchowski M S, Eckstein J N and Bozovic I 1997 *Phys. Rev.* B **55** 5873
[9] Ziese M and Sena S P 1998 *J. Phys.: Condens. Matter* **10** 2727
[10] Amaral V S *et al* 2000 *J. Appl. Phys.* **87** 5570
[11] Bibes M, Gorbenko O Yu, Martínez B, Kaul A R and Fontcuberta J 2000 *J. Magn. Magn. Mater.* **211** 47
[12] Bibes M, Martínez B, Fontcuberta J, Trtík V, Ferrater C, Sánchez F, Varela M, Hiergeist R and Steenbeck K 2000 *J. Magn. Magn. Mater.* **211** 206
[13] Ziese M 2002 *Rep. Prog. Phys.* **65** 143
[14] Berger L 1970 *Phys. Rev.* B **2** 4459
[15] Matl P, Ong N P, Yan Y F, Li Y Q, Studebaker D, Baum T and Doubinina G 1998 *Phys. Rev.* B **57** 10248
[16] Jakob G, Martin F, Westerburg W and Adrian H 1998 *Phys. Rev.* B **57** 10252
[17] Ziese M 1999 *Phys. Rev.* B **60** R738
[18] Lyanda-Geller Y, Chun S, Salamon M, Goldbart P, Han P, Tomioka Y, Asamitsu A and Tokura Y 2001 *Phys. Rev.* B **63** 184426
[19] Calderón M J and Brey L 2001 *Phys. Rev.* B **63** 054421
[20] Lark-Horovitz K and Johnson V 1959 *Methods of Experimental Physics* vol 6B (New York: Academic) p 145
[21] Núñez-Regueiro J and Kadin A 1998 *J. Phys. D: Appl. Phys.* **31** L1
[22] Laukhin V *et al* 2005 *J. Phys. D: Appl. Phys.* at press
[23] Pickett W E and Singh D J 1997 *Phys. Rev.* B **55** R8642
[24] Yang H C, Wang L M and Horng H E 2001 *Phys. Rev.* B **64** 174415
[25] Asamitsu A and Tokura Y 1998 *Phys. Rev.* B **58** 47
[26] Gordon I *et al* 2000 *Phys. Rev.* B **62** 11633